H. Canbolat

D. Dawson

C. Rahn[1]
Assoc. Mem. ASME

S. Nagarkatti

Center for Advanced Manufacturing,
Clemson University,
Clemson, SC 29634-0915

Adaptive Boundary Control of Out-of-Plane Cable Vibration

This paper develops active controllers for the out-of-plane vibration of a flexible cable using boundary actuators and sensors. An exact model knowledge controller exponentially stabilizes the cable displacement assuming known system parameters. An adaptive controller asymptotically stabilizes the cable displacement while compensating for parametric uncertainty in the actuator mass and cable tension. The performance of the controllers is experimentally demonstrated.

1 Introduction

Cables are used in many engineering applications due to their inherent low weight, flexibility, strength, and storability. The transverse stiffness of a cable depends on its tension and length, however, so long, sagged cables can vibrate excessively in response to relatively small disturbances. This vibration degrades the performance of the cable system and ultimately leads to failure.

To understand cable structure vibration, many researchers have developed sophisticated modeling and analysis techniques (see Irvine, 1981, for a review). Small sag approximation techniques (Soler, 1970), lumped parameter models (West et al., 1975), finite element techniques (Fried, 1982), and Galerkin methods (Perkins and Mote, 1987) represent several approaches used to predict the behavior of cables in a variety of applications. These analysis tools motivate the development of passive vibration control methods, including increase of the cable tension and/or addition of damping mechanisms. Increased tension induces high stress, however, reducing the cable life. Cable dampers can reduce the resonant forced response but may have little effect on the transient response.

Active vibration control has only recently been applied to cable systems. Cost and/or feasibility of this method often dictates that control actuators be located at the boundaries of the cable span. Fujino et al. (1993) developed axial boundary force control laws for a single-mode cable model and experimentally demonstrated a large reduction in peak resonant response. Fujino and Susumpow (1995) extended this approach to multiple cable modes. Baicu et al. (1996a) developed a linear feedback controller for the out-of-plane vibration of a distributed cable model. The proposed controller consisted of boundary position, velocity, and slope feedback. The cable position was proven to be stable under the proposed control. Simulation and experimental results demonstrated very good vibration damping.

Researchers have also applied boundary control to many other flexible systems. The motion of flexible gantry robots can be regulated with boundary control (Luo et al., 1995). Boundary controllers have been developed to stabilize the vibration associated with flexible beam-like structures (e.g., aircraft wings, robot links, or space structures) (Chen et al., 1987; Morgül, 1991; Rahn and Mote, 1993; Canbolat et al., 1997). Related boundary control work for string-like dynamic models can also be found in Morgül (1994) and Shahruz and Krishna (1996). Interestingly, the control structure proposed in this paper reduces to a form which is similar to the one given in Morgül (1994) if the cable tension is assumed to be constant.

In this paper, we develop new control strategies for the distributed cable model given in Baicu et al. (1996a). Specifically, we develop a model-based controller that exponentially stabilizes the displacement of the cable given exact knowledge of the mechanical system parameters and measurements of the slope, slope-rate, and velocity at the cable's actuated boundary. We then illustrate how the exact model knowledge controller can be redesigned as an adaptive controller which asymptotically stabilizes the cable displacement while compensating for parametric uncertainty. The control approach differs from the previous work in that (i) the stability analysis utilizes more intuitive mathematical tools to illustrate the exponential and asymptotic stability results, (ii) a new Lyapunov-like function is crafted to deal with the spatially varying tension, and (iii) adaptive nonlinear control techniques are applied.

2 Mathematical Model

Figure 1(*b*) shows a cable sagging under gravity loading. The cable vibrates perpendicular to the plane formed by the equilibrium cable configuration. Figure 1(*a*) shows the out-of-plane displacement $U(S, T)$ where S is the arc length coordinate and T is time. The left boundary is pinned and the right boundary is free to translate in the out-of-plane direction. A control force $F(T)$ applies in the out-of-plane direction at the left boundary. From Baicu et al. (1996a), the linearized out-of-plane equation of motion, valid for small amplitude motion, is

$$\rho A U_{TT} - [P(S) U_S]_S = 0, \tag{1}$$

where ρA is the cable mass/length and subscripts indicate partial differentiation. The equilibrium tension

$$P(S) = \sqrt{P_0^2 + \left[\rho A g\left(S - \frac{L}{2}\right)\right]^2}, \tag{2}$$

where P_0 is the midspan ($S = L/2$) or horizontal component of the cable tension, g is the acceleration due to gravity, and L is the cable length. The pinned boundary condition at $S = 0$ is

$$U(0, T) = 0, \tag{3}$$

and the controlled boundary condition at $S = L$ is

[1] To whom correspondence should be addressed. e-mail: cdrahn@eng.clemson.edu.

Contributed by the Applied Mechanics Division of THE AMERICAN SOCIETY OF MECHANICAL ENGINEERS for publication in the ASME JOURNAL OF APPLIED MECHANICS.

Discussion on the paper should be addressed to the Technical Editor, Professor Lewis T. Wheeler, Department of Mechanical Engineering, University of Houston, Houston, TX 77204-4792, and will be accepted until four months after final publication of the paper itself in the ASME JOURNAL OF APPLIED MECHANICS.

Manuscript received by the ASME Applied Mechanics Division, Aug. 27, 1997; final revision, May 11, 1998. Associate Technical Editor: A. A. Ferri.

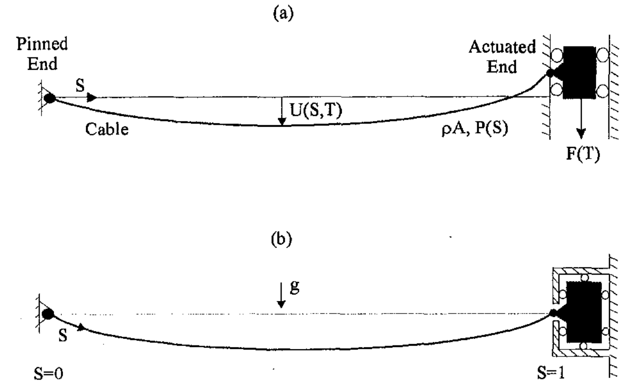

Fig. 1 Schematic diagram of the cable system: (*a*) top view, (*b*) side view

$$MU_{TT} + P(S)U_S - F_f = F, \quad (4)$$

where M is the actuator mass and $F_f(U_T(L, T))$ models friction and/or damping in the actuator.

Nondimensionalization simplifies the control development. Substitution of the nondimensional variables

$$s = \frac{S}{L}; \quad t = T\sqrt{\frac{g}{L}}; \quad u = \frac{U}{L}; \quad m = \frac{M}{\rho AL}; \quad f = \frac{F}{\rho AgL};$$

$$p(s) = \frac{P(S)}{\rho AgL} = \sqrt{p_0^2 + \left(s - \frac{1}{2}\right)^2}; \quad p_0 = \frac{P_0}{\rho AgL} \quad (5)$$

into Eq. (1) yields

$$u_{tt}(s, t) - [p(s)u_s(s, t)]_s = 0 \quad (6)$$

with boundary conditions[2]

$$u(0, t) = 0, \quad (7)$$

$$mu_{tt}(1, t) + p(1)u_s(1, t) + Y(u_t(1, t))\phi = f(t), \quad (8)$$

where $Y(u_t(1, t))\phi$ is the nondimensionalized F_f linearly parameterized as a known regression matrix $Y(u_t(1, t)) \in \Re^{1\times q}$ multiplied by a constant parameter vector $\phi \in \Re^{q\times 1}$. For example, an actuator with viscous damping b and Coulomb friction μ has

$$Y(u_t(1, t)) = [u_t(1, t) \quad \text{sgn}\,(u_t(1, t))], \quad (9)$$

$$\phi^T = [b \quad \mu], \quad (10)$$

where sgn $(\cdot)$ is the signum function. We will also assume that $Y(u_t(1, t))$ remains bounded $\forall t \in [0, \infty)$ if $u_t(1, t)$ is bounded $\forall t \in [0, \infty)$.

3 Control Formulation

In this section of the paper, we present two control strategies that stabilize the distributed cable vibration Eqs. (6)–(8) using the boundary control force $f(t)$. First, we define the structure and closed-loop boundary dynamics of a controller that requires exact knowledge of the system parameters. Using a Lyapunov-like stability analysis, we prove this exact model knowledge controller drives the cable displacement to zero exponentially fast. Dynamic compensation using an adaptive controller allows implementation without knowledge of the cable tension and actuator mass. This controller, however, provides only asymptotic regulation of the cable displacement.

[2] The pinned boundary conditions of (7) imply that $u_t(0, t) = 0$.

3.1 Exact Model Knowledge Control Law. The exact model knowledge control law is defined as follows:

$$f = -mu_{st}(1, t) + p(1)u_s(1, t) - k_s(u_t(1, t) + u_s(1, t)) + Y(u_t(1, t))\phi, \quad (11)$$

where k_s is a positive control gain. Note that the actuator mass m and tension $p(1)$ must be known to implement this controller.

THEOREM 1. *Given the field equation of (6) and the boundary conditions given by (7) and (8), the boundary controller given by (11) ensures that the cable displacement is regulated exponentially fast in the following sense,*

$$|u(s, t)| \le \sqrt{\frac{2\lambda_2}{\lambda_1 p}\kappa_o \exp\left(-\frac{\lambda_3}{\lambda_2}t\right)} \quad \forall s \in [0, 1], \quad (12)$$

where λ_1, λ_2, and λ_3 are positive bounding constants, the positive constant κ_o is given by

$$\kappa_o = \frac{1}{2}\int_0^1 u_t^2(\sigma, 0)d\sigma + \frac{1}{2}\int_0^1 p(\sigma)u_\sigma^2(\sigma, 0)d\sigma + (u_t(1, 0) + u_s(1, 0))^2, \quad (13)$$

if the controller gain k_s defined in (11) satisfies

$$k_s > \frac{p(1)}{2}. \quad (14)$$

Proof. To facilitate the stability proof, we first define an auxiliary tracking signal

$$\eta(t) = u_t(1, t) + u_s(1, t). \quad (15)$$

After differentiating (15) with respect to time, multiplying the resulting expression by m, and then substituting the right-hand side of (8) for $mu_{tt}(1, t)$, we have

$$m\dot{\eta} = mu_{st}(1, t) - p(1)u_s(1, t) - Y(u_t(1, t))\phi + f, \quad (16)$$

where $\dot{\eta} = \eta_t$. After substituting (11) into (16), we obtain the following closed-loop dynamics on the boundary:

$$m\dot{\eta} = -k_s\eta. \quad (17)$$

Remark 1. The following inequalities are used in the proof. First, the boundary condition Eq. (7) allows formulation of (see Hardy et al., 1959)

$$u^2(s, t) \le \int_0^1 u_\sigma^2(\sigma, t)d\sigma \quad \forall s \in [0, 1]. \quad (18)$$

Second, using the triangle inequality we have

$$-(z^2 + y^2) \le |zy| \quad z^2 + y^2 \ge zy \quad \forall z, y \in \Re. \quad (19)$$

To prove Eq. (12), we begin with the following function:

$$V(t) = E_s(t) + \tfrac{1}{2}m\eta^2(t) + E_c(t). \quad (20)$$

The cable vibration energy is

$$E_s(t) = \frac{1}{2}\int_0^1 u_t^2(\sigma, t)d\sigma + \frac{1}{2}\int_0^1 p(\sigma)u_\sigma^2(\sigma, t)d\sigma, \quad (21)$$

and the crossing term is

$$E_c(t) = 2\beta\int_0^1 \gamma(\sigma)u_t(\sigma, t)u_\sigma(\sigma, t)d\sigma, \quad (22)$$

where β is a positive design constant and the weighting function

$$\gamma(s) = \frac{h(s)}{2p_0}\left[\arctan\left(\frac{2s-1}{2p_0}\right) + p_0 \ln(2s - 1 + h(s)) + \arctan\frac{1}{2p_0} + p_0 \ln(\sqrt{4p_0^2+1} - 1)\right] \quad (23)$$

with

$$h(s) = \sqrt{4p_0^2 + 4s^2 - 4s + 1}.$$

If the design constant β is selected according to

$$\beta < \frac{\min\{1, p_0\}}{4\gamma(1)}, \quad (24)$$

we can formulate the following upper and lower bound on $V(t)$ (see Lemma A.1 in the Appendix)

$$\lambda_1(E_s(t) + \eta^2(t)) \le V(t) \le \lambda_2(E_s(t) + \eta^2(t)), \quad (25)$$

where the positive constants λ_1 and λ_2 are

$$\lambda_1 = \min\left\{1 - \frac{4\beta\gamma(1)}{\min\{1, p_0\}}, \frac{m}{2}\right\},$$

$$\lambda_2 = \max\left\{1 + \frac{4\beta\gamma(1)}{\min\{1, p_0\}}, \frac{m}{2}\right\}. \quad (26)$$

After differentiating (20) with respect to time and substituting (6), (7), and (17), we obtain the following upper bound on the time derivative of $V(t)$ (See Lemma A.2 in the Appendix):

$$\dot{V}(t) \le -\lambda_3(E_s(t) + \eta^2(t)), \quad (27)$$

where the positive constant[3] λ_3 is defined by

$$\lambda_3 = \min\left\{2\beta, k_s - \frac{p(1)}{2}\right\}. \quad (28)$$

Remark 2. The structure of the weighting function $\gamma(s)$ defined in (23) has been crafted to facilitate the construction of the inequalities given in (25) and (27).

From (25) and (27), we obtain the following upper bound for the time derivative of $V(t)$

$$\dot{V}(t) \le -\frac{\lambda_3}{\lambda_2} V(t), \quad (29)$$

whose solution yields

$$V(t) \le V(0)\exp\left(-\frac{\lambda_3}{\lambda_2}t\right) \le \lambda_2\kappa_o \exp\left(-\frac{\lambda_3}{\lambda_2}t\right), \quad (30)$$

where Eq. (25) has been utilized to formulate the inequality on the right-hand side of Eq. (30) and the positive constant κ_o is defined in Eq. (13). In addition, we use Eqs. (18), (21), and (25) to formulate the following inequality:

$$\frac{p_0}{2}u^2(x, t) \le \frac{1}{2}\int_0^1 p(\sigma)u_\sigma^2(\sigma, t)d\sigma \le E_s(t) \le \frac{1}{\lambda_1}V(t) \quad \forall x \in [0, 1]. \quad (31)$$

The inequality given in Eq. (12) now directly follows by combining Eqs. (30) and (31) and then using Eqs. (15) and (21). □

Remark 3. Since the proposed control strategies are relatively simple, smooth functions, we have assumed existence of solution for the dynamics given by (6) through (8) under the proposed control. To illustrate bounded-input, bounded-output stability for the closed-loop system, we invoke the following reasonable assumption: The distributed variable $u(s, t)$, and its time derivative $u_t(s, t)$, belong to a space of functions which has the following properties: (i) if $u(s, t)$ is bounded $\forall t \in [0, \infty)$ and $\forall s \in [0, 1]$, then $u_s(s, t)$ and $u_{ss}(s, t)$ are bounded $\forall t \in [0, \infty)$ and $\forall s \in [0, 1]$, and (ii) if the kinetic energy for the mechanical system of (6) through (8)

$$\frac{1}{2}\int_0^1 u_t^2(\sigma, t)d\sigma + \frac{1}{2}mu_t^2(1, t) \quad (32)$$

is bounded then $u_t(s, t)$ and $u_{st}(s, t)$ are bounded for $\forall t \in [0, \infty)$ and $\forall s \in [0, 1]$.

Remark 4. From (20) and (30), we can state that $E_s(t)$ and $\eta(t)$ are bounded $\forall t \in [0, \infty)$. Since $E_s(t)$ is bounded $\forall t \in [0, \infty)$, we can use (21), (18), and the properties discussed in Remark 3 to state that $u(s, t)$, $u_s(s, t)$, and $u_{ss}(s, t)$ are bounded $\forall t \in [0, \infty)$ and $\forall s \in [0, 1]$. Since $\eta(t)$ and $u_s(1, t)$ are bounded $\forall t \in [0, \infty)$, we can use (15) to state that $u_t(1, t)$ is bounded $\forall t \in [0, \infty)$; hence, the kinetic energy of the mechanical system defined in (32) is bounded $\forall t \in [0, \infty)$. Since the kinetic energy is bounded $\forall t \in [0, \infty)$, we can use the properties discussed in Remark 3 to state that $u_t(s, t)$ and $u_{st}(s, t)$ are bounded for $\forall t \in [0, \infty)$ and $\forall s \in [0, 1]$. From the above information, we can now state that all of the signals in the control of (11) and the mechanical system given by (6) through (8) remain bounded $\forall t \in [0, \infty)$ during closed-loop operation.

3.2 Adaptive Control Law. In this subsection, we redesign the exact model knowledge controller (11) to compensate for *constant* parametric uncertainty while asymptotically stabilizing the mechanical model given by (6) through (8). The adaptive control law is

$$f = -W\hat{\theta} - k_s\eta, \quad (33)$$

where $W(t) \in \Re^{1\times(q+2)}$ is a known regression matrix and $\hat{\theta}(t) \in \Re^{(q+2)\times 1}$ is a dynamic parameter estimate vector:

$$W = [u_{st}(1, t), -u_s(1, t), -Y(u_t(1, t))],$$

$$\hat{\theta} = [\hat{m}, \widehat{p(1)}, \hat{\phi}^T]^T. \quad (34)$$

The parameter estimate vector introduced in (33) is updated online according to

$$\dot{\hat{\theta}} = \Gamma W^T\eta, \quad (35)$$

where $\Gamma \in \Re^{(q+2)\times(q+2)}$ is a constant, diagonal gain matrix with elements $\Gamma_i > 0$.

THEOREM 2. *Given the field equation of (6) and the boundary conditions given by (7) and (8), the boundary controller given by (33) and (35) ensures that the cable displacement is regulated asymptotically fast in the following sense:*

$$\lim_{t\to\infty} |u(s, t)| = 0 \quad \forall s \in [0, 1], \quad (36)$$

where the controller gain k_s defined in (33) must be selected to satisfy (14).

Proof. After differentiating (15) with respect to time, multiplying the resulting expression by m, and then substituting the right-hand side of (8) for $mu_{tt}(L, t)$, we have

$$m\dot{\eta} = W\theta + f, \quad (37)$$

where $W(t)$ was defined in (34) and $\theta \in R^{(q+2)\times 1}$ is the unknown constant parameter vector defined as

[3] The controller gain k_s must satisfy (14) to ensure that λ_3 is positive.

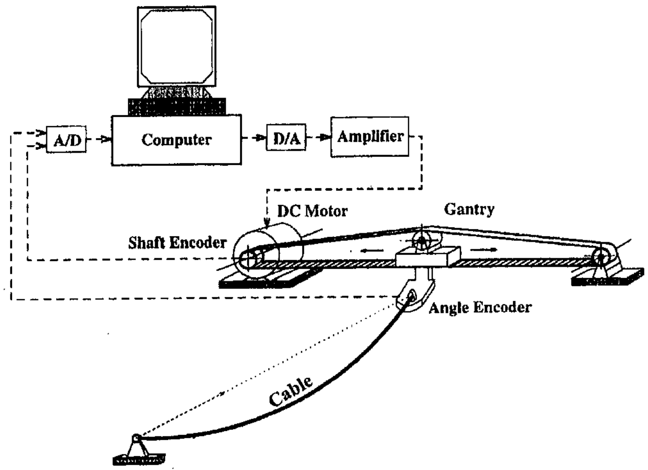

Fig. 2 Schematic diagram of the experimental setup

$$\theta = [m \quad p(1) \quad \phi^T]^T. \tag{38}$$

After substituting (33) into (37), we obtain the following closed-loop dynamics on the boundary:

$$m\dot{\eta} = -k_s\eta + W\tilde{\theta},$$
$$\dot{\tilde{\theta}} = -\Gamma W^T\eta, \tag{39}$$

where $\tilde{\theta}(t) = \theta - \hat{\theta}(t) \in \Re^{(q+2)\times 1}$ is the parameter estimate error vector, and (35) has been used to obtain the parameter estimation error dynamics.

To prove Eq. (36), we begin with the following function:

$$V_a(t) = V(t) + \tfrac{1}{2}\tilde{\theta}^T(t)\Gamma^{-1}\tilde{\theta}(t), \tag{40}$$

where $V(t)$ was defined in (20). If the design constant β of (22) is selected to be sufficiently small, Lemma A.1 can be used to show

$$\lambda_{1a}[E_s(t) + \eta^2(t) + \|\tilde{\theta}(t)\|^2] \le V_a(t) \le \lambda_{2a}[E_s(t) + \eta^2(t) + \|\tilde{\theta}(t)\|^2], \tag{41}$$

where the positive constants λ_{1a} and λ_{2a} are defined by

$$\lambda_{1a} = \min\left\{1 - \frac{4\beta\gamma(1)}{\min\{1, \rho\}}, \frac{m}{2}, \frac{1}{2}\min\{1/\Gamma_i\}\right\},$$

$$\lambda_{2a} = \max\left\{1 + \frac{4\beta\gamma(1)}{\max\{1, \rho\}}, \frac{m}{2}, \frac{1}{2}\max\{1/\Gamma_i\}\right\}.$$

After differentiating (40) with respect to time, substituting (6), (7), and (39), and using Lemma A.2, we obtain the following upper bound for the time derivative of $V_a(t)$:

$$\dot{V}_a(t) \le -\lambda_3(E_s(t) + \eta^2(t)) \triangleq g_a(t), \tag{42}$$

where λ_3 was defined in (28). We can now use (41), (42), and a similar argument as that outlined in Remark 3 to state that all of the signals in the control of (33) and (35) are bounded and that all of the signals in the mechanical system given by (6) through (8) remain bounded.

After differentiating the right-hand side of (42) with respect to time, we have

$$\dot{g}_a(t) = -\lambda_3(\dot{E}_s(t) + 2\eta(t)\dot{\eta}(t)). \tag{43}$$

Since we illustrated how all of the system signals remain bounded $\forall t \in [0, \infty)$, we can use (53) and (39) to show that $\dot{E}_s(t)$ and $\dot{\eta}(t)$ are bounded $\forall t \in [0, \infty)$; hence, we can see from (43) that the time derivative of the right-hand side of (42) is also bounded $\forall t \in [0, \infty)$. We can now invoke Lemma A.3 in the Appendix to the right-hand side of (42) to show that

$$\lim_{t\to\infty} E_s(t), \eta(t) = 0. \tag{44}$$

We can now use the result given by (44) and the inequality-type bound developed in (31) to state the result given by (36). □

Remark 5. It should be noted that several extensions to the basic controllers given in the previous sections can be devel-

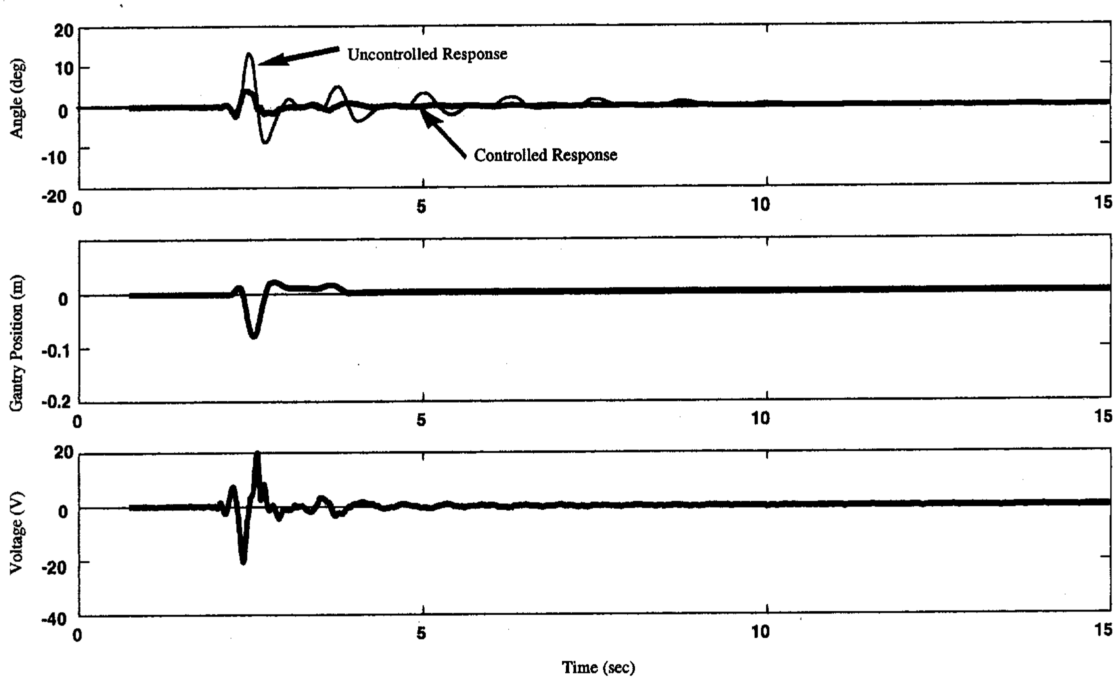

Fig. 3 Experimental results—exact model knowledge controller

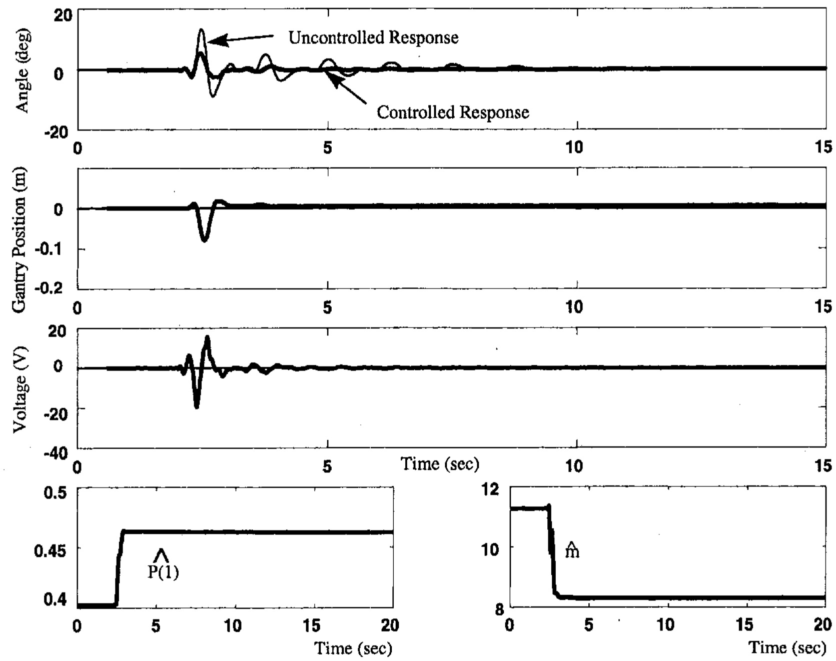

Fig. 4 Experimental results—adaptive controller

oped. For example, an additional gain constant in the definition of the tracking variable $\eta(t)$ defined in (15) can be added. Specifically, we can redefine the exact model knowledge input control force originally defined in (11) as follows:

$$f = -m\alpha u_{st}(1, t) + p(1)u_s(1, t) - k_s\eta + Y(u_t(1, t))\phi, \quad (45)$$

where α is a positive controller gain, and the variable $\eta(t)$ originally defined in (15) is now defined as follows:

$$\eta = u_t(1, t) + \alpha u_s(1, t). \quad (46)$$

As illustrated in Canbolat et al. (1997) for a similar mechanical system, we can slightly modify the arguments outlined in Remark 3 and the proof of Theorem 1 to show that all of the signals in the control and the mechanical system remain bounded and to state a similar exponential stability result as that given by (12). By following the adaptive control technique given in the previous section, we can also redesign the controller given by (45) as an adaptive controller which compensates for parametric uncertainty and achieves asymptotic displacement regulation.

4 Experimental Results

The proposed controller was implemented on a cable control system designed and built in-house (see Fig. 2). A braided polyester rope, pinned at one end, and connected to a horizontally translating gantry at the other end was used for the experiments. A brushed DC motor (Baldor model 3300) was coupled to the gantry using a timing belt. Two 1000-count rotary encoders (Hohner) were used to measure the gantry position and the cable departure angle. A mounting bracket attached to the gantry aligned the departure angle encoder axis with the normal (in-plane) direction. Thus, the measured encoder rotation caused by cable motion corresponded to out-of-plane slope at the controlled boundary $u_s(1, t)$. A 486 ISA-based PC hosting a Texas Instruments TMS320C30 digital signal processing board served as the computational engine. An encoder interface card (Integrated Motions, Inc., Model DS-2) allowed for quadrature extrapolation of the encoder signals. The DS2 board also supported two channels of 16-bit ADCs and DACs. The linear and angular velocities were obtained by applying a backwards difference algorithm to the position and angle signals, respectively. To eliminate quantization noise, the velocity signals were filtered using a second-order digital filter. To test the response of the proposed controller, the cable was perturbed using a repeatable displacement input disturbance near the pinned end. As defined in (5), the parameter values for the mechanical system were determined via standard test procedures to be as follows:

$$M = 3.229 \text{ kg} \quad L = 2.69 \text{ m} \quad \rho A = 0.085 \text{ kg/m}$$
$$g = 9.81 \text{ m/s}^2 \quad P_0 = 0.127 \text{ N}$$

$$m = 14.1 \quad p_0 = 0.056 \quad p(1) = 0.503$$

Two experiments were conducted to test the performance of the proposed controller. First, the exact model knowledge controller given by (45) was implemented using the following settings:

$$k_s = 5.0 \quad \alpha = 4.0 \quad Y(u_t(1, t))\phi = 0.$$

The results of these experiments appear in Fig. 3. As is clear from the figure, the cable system exhibits excellent transient response under the proposed controller. The uncontrolled swinging of the cable to the same input is shown for comparison purposes. The gantry position and the voltage signals are also shown. It should also be noted that the $Y(u_t(1, t))\phi$ term could have been used to model static friction on the rail of the actuator; however, the feedback portion of the controller seemed to adequately compensate for friction in our experiment.

The adaptive version of (45) was implemented with the update law given by (35) and the parameter estimates initialized to 80 percent of their nominal values. The best performance was achieved using the following settings:

$$k_s = 5.0 \quad \alpha = 4.0 \quad Y(u_t(1, t))\phi = 0 \quad \Gamma = \text{diag}\{5, 2\}.$$

The results of these experiments appear in Fig. 4. In the first subplot of Fig. 4, the transient performance of the adaptive controller to the disturbance is compared to the uncontrolled swinging of the cable for the same input. Subsequent subplots show the gantry position and the voltage signals. As is clear from the figure, the estimates for the parameters m and $p(1)$ remain bounded during closed-loop operation.

Remark 6. The input control force at the actuator is actually applied by rescaling this force as a desired motor torque. The desired motor torque is then achieved by using a high-gain current feedback loop (recall for the brushed DC motor that $\tau_{\text{motor}} \propto I$ where I is the motor current). The current feedback loop and the torque-force conversion are incorporated into the control software and power is supplied to the motor by the single-channel linear power amplifier which is capable of outputting up to 1000 W at 100 V with a power bandwidth of 0 to 40 KHz. It should be noted that the backstepping paradigm (Kokotovic, 1992) allows electrical dynamics to be incorporated in the overall control solution for this class of hybrid partial/ordinary differential equation problems as illustrated in Baicu et al. (1996b).

Remark 7. Dimensional quantities are used in the experiment so the control force is scaled according to (5) (i.e., $F = f\rho AgL$). This implies that the weight of the cable must be known in order to implement the controllers.

5 Conclusion

In this paper, we develop new boundary control strategies for a flexible cable with actuator dynamics. The control structure differs substantially from the controller in Baicu et al. (1996a) because different signals are sensed.[4] While the controller given in Baicu et al. (1996a) only provides for bounded-input, bounded-output stability, the proposed exact model knowledge controller exponentially stabilizes the position of the cable and the adaptive controller asymptotically stabilizes the position of the cable and compensates for parametric uncertainty in the cable tension and actuator mass. The experimental results are similar to those of Baicu et al. (1996a), demonstrating fast transient decay under the proposed control.

Acknowledgment

This work is supported in part by the U.S. National Science Foundation Grants DMI-9457967, DDM-931133269, DMI-9622220, the Office of Naval Research URI-3139-YIP01, the Square D Corporation, the Union Camp Corporation, the AT&T Foundation, and Mersin University, Mersin, Turkey.

References

Baicu, C. F., Rahn, C. D., and Nibali, B. D., 1996a, "Active Boundary Control of Elastic Cables: Theory and Experiment," *Journal of Sound and Vibration*, Vol. 198, No. 1, pp. 17–26.

Baicu, C. F., Rahn, C. D., and Dawson, D., 1996b, "Boundary Control of a Flexible Link Electrically Driven Gantry Robot," *Active Control of Vibration and Noise*, ASME, New York, pp. 109–115.

Canbolat, H., Dawson, D., and Rahn, C., 1997, "Boundary Control of a Cantilevered Flexible Beam with Point-Mass Dynamics at the Free End," *Proc. of the 38th AIAA/ASME/ASCE/AHS/ASC Structures, Structural Dynamics, and Materials Conference and the AIAA/ASME/AHS Adaptive Structures Forum*, Part 2, Kissimmee, FL, Apr., pp. 1589–1598.

Chen, G., Delfour, M., Krall, A., and Payre, G., 1987, "Modeling, Stabilization, and Control of Serially Connected Beams," *SIAM Journal of Control and Optimization*, Vol. 25, No. 3, pp. 526–546.

Fried, I., 1982, "Large Deformation Static and Dynamic Finite Element Analysis of Extensible Cables," *Computers and Structures*, Vol. 15, pp. 315–319.

Fujino, Y., Warnitchai, P., and Pacheco, B., 1993, "Active Stiffness Control of Cable Vibration," ASME JOURNAL OF APPLIED MECHANICS, Vol. 60, pp. 948–953.

Fujino, Y., and Susumpow, T., 1995, "Active Control of Multimodal Cable Vibrations by Axial Support Motion," *Smart Materials and Structures*, Vol. 4, pp. A41–A51.

Hardy, G., Littlewood, J., and Polya, G., 1959, *Inequalities*, Cambridge University Press, Cambridge, UK.

Irvine, H., 1981, *Cable Structures*, MIT Press, Cambridge, MA.

Kokotovic, P., 1992, "The Joy of Feedback: Nonlinear and Adaptive," *IEEE Control Systems Magazine*, Vol. 12, June, pp. 7–17.

Luo, Z., Kitamura, N., and Guo, B., 1995, "Shear Force Feedback Control of Flexible Robot Arms," *IEEE Transactions on Robotics and Automation*, Vol. 11, No. 5, pp. 760–765.

Morgül, Ö., 1991, "Orientation and Stabilization of a Flexible Beam Attached to a Rigid Body: Planar Motion," *IEEE Transactions on Automatic Control*, Vol. 36, No. 8, pp. 953–962.

Morgül, Ö., Rao, B., and Conrad, F., 1994, "On the Stabilization of a Cable with a Tip Mass," *IEEE Transactions on Automatic Control*, Vol. 39, No. 10, pp. 2140–2145.

Perkins, N., and Mote, C., 1987, "Three-dimensional Vibration of Travelling Elastic Cables," *Journal of Sound and Vibration*, Vol. 114, No. 2, pp. 325–340.

Rahn, C., and Mote, C., 1993, "Axial Force Stabilization of Transverse Beam Vibration," *Vibration and Control of Mechanical Systems*, ASME, New York, pp. 29–34.

Shahruz, S. M., and Krishna, L. G., 1996, "Boundary Control of Nonlinear String," *Proc. of the ASME Dynamics Systems and Control Division*, ASME, New York, pp. 831–835.

Slotine, J., and Li, W., 1991, *Applied Nonlinear Control*, Prentice-Hall, Englewood Cliffs, NJ.

Soler, A., 1970, "Dynamic Response of Single Cable with Initial Sag," *Journal of the Franklin Institute*, Vol. 190, pp. 377–387.

West, H., Geschwinder, L., and Suchoski, J., 1975, "Natural Vibrations of Suspension Cables," *Journal of the Structural Division, ASCE*, Vol. 101, pp. 2277–2291.

APPENDIX

Stability Lemmas

LEMMA A.1. *The non-negative function given by (20) can be upper and lower bounded as given by (25).*

Proof. First, note that (19) can be used to bound $E_c(t)$ of (22) as follows:

$$E_c = 2\beta \int_0^1 \gamma(\sigma) u_t u_\sigma d\sigma \leq 2\beta\gamma(1) \int_0^1 (u_t^2 + u_\sigma^2) d\sigma,$$

$$\leq \frac{4\beta\gamma(1)}{\min(1, p_0)} \left[\frac{1}{2} \int_0^1 (u_t^2 + p(\sigma) u_\sigma^2) d\sigma \right], \tag{47}$$

where we have used the facts that $p(s)$ is minimum at $s = \frac{1}{2}$ for $s \in [0, 1]$ and that $\gamma(s)$ of (23) is maximum at $s = 1$ for $s \in [0, 1]$. We can now use (21) and (47) to establish the following inequality:

$$-\frac{4\beta\gamma(1)}{\min(1, p_0)} E_s \leq E_c \leq \frac{4\beta\gamma(1)}{\min(1, p_0)} E_s; \tag{48}$$

hence, if β is selected according to (24), we have

$$0 \leq \left(1 - \frac{4\beta\gamma(1)}{\min\{1, p_0\}}\right) E_s \leq E_s + E_c$$

$$\leq \left(1 + \frac{4\beta\gamma(1)}{\min\{1, p_0\}}\right) E_s. \tag{49}$$

Given the structure of $V(t)$ defined in (20) and the inequality given by (49), the inequality given by (25) is obvious.

LEMMA A.2. *The time derivative of the nonnegative function given by (20) can be upper bounded as given by (27).*

Proof. After differentiating (20) with respect to time, we have

$$\dot{V} = \dot{E}_s + \dot{E}_c - k_s \eta^2, \tag{50}$$

where (17) has been used. To determine $\dot{E}_s(t)$ in (50), we differentiate (21) with respect to time to obtain

$$\dot{E}_s = \int_0^1 u_t [p(\sigma) u_\sigma]_\sigma d\sigma + \int_0^1 p(\sigma) u_\sigma u_{\sigma t} d\sigma, \tag{51}$$

where (6) has been used. If we integrate the first term on the right-hand side of (51) by parts, we obtain

$$\dot{E}_s = p(1) u_t(1, t) u_s(1, t) - p(0) u_t(0, t) u_s(0, t). \tag{52}$$

After applying the boundary conditions given in (7) to (52), we have

$$\dot{E}_s = p(1) u_t(1, t) u_s(1, t), \tag{53}$$

[4] The controller given in Baicu et al. (1996a) requires measurement of boundary position, velocity, and the slope while the proposed controller requires measurement of the boundary velocity, slope, and slope rate.

which can be written as

$$\dot{E}_s = -\frac{p(1)}{2}(u_t^2(1,t) + u_s^2(1,t)) + \frac{p(1)}{2}\eta^2 \quad (54)$$

upon application of (15).

To determine $\dot{E}_c(t)$ in (50), we differentiate (22) with respect to time as follows:

$$\dot{E}_c = A_1 + A_2, \quad (55)$$

where

$$A_1 = 2\beta \int_0^1 \gamma(\sigma) u_t u_{\sigma t} d\sigma,$$

$$A_2 = 2\beta \int_0^1 \gamma(\sigma) u_\sigma [p(\sigma) u_\sigma]_\sigma d\sigma, \quad (56)$$

after using (6) in the expression for A_2. After integrating the expression for A_1 given by (56) by parts, we obtain

$$A_1 = 2\beta \left(\gamma(1) u_t^2(1,t) - \int_0^1 \gamma_\sigma(\sigma) u_t^2 \, d\sigma \right) - 2\beta \int_0^1 \gamma(\sigma) u_{\sigma t} u_t d\sigma, \quad (57)$$

where we have used the fact that $\gamma(0) = 0$. After noting that the last term in (57) is equal to A_1, we can write (57) as follows:

$$A_1 = \beta \left(\gamma(1) u_t^2(1,t) - \int_0^1 \gamma_\sigma(\sigma) u_t^2 \, d\sigma \right), \quad (58)$$

where $\gamma_s(s)$ is explicitly given by

$$\gamma_s(s) = \frac{8s-4}{4p_0 h(s)} \left[\arctan\left(\frac{2s-1}{2p_0}\right) + p_0 \ln(2s - 1 + h(s)) - \arctan\frac{1}{2p_0} + p_0 \ln(\sqrt{4p_0^2+1} - 1) \right] + \frac{h(s)}{2p_0} \left(\frac{1}{p_0\left(1 + \frac{(2s-1)^2}{4p_0^2}\right)} + \frac{p_0\left(2 + \frac{8s-4}{2h(s)}\right)}{2s - 1 + h(s)} \right).$$

It can be shown that $\gamma_s(s) \geq 1$ for $s \in [0, 1]$; hence, we can utilize (58) to construct the following upper bound for A_1:

$$A_1 \leq \beta \left(\gamma(1) u_t^2(1,t) - \int_0^1 u_t^2 \, d\sigma \right). \quad (59)$$

After integrating the expression for A_2 given by (56) by parts, we obtain

$$A_2 = 2\beta \left(\gamma(1) p(1) u_s^2(1,t) - \int_0^1 \gamma_\sigma(\sigma) p(\sigma) u_\sigma^2 \, d\sigma - \int_0^1 \gamma(\sigma) p(\sigma) u_\sigma u_{\sigma\sigma} d\sigma \right), \quad (60)$$

where we have used the fact that $\gamma(0) = 0$. After noting that the expression for A_2 given by (56) can be expanded into the following form,

$$A_2 = 2\beta \left(\int_0^1 \gamma(\sigma) u_\sigma^2 p_\sigma(\sigma) d\sigma + \int_0^1 \gamma(\sigma) p(\sigma) u_\sigma u_{\sigma\sigma} d\sigma \right), \quad (61)$$

we can combine (60) and (61) to eliminate the last term in (60) as follows:

$$A_2 = \beta \left(\gamma(1) p(1) u_s^2(1,t) - \int_0^1 [\gamma_\sigma(\sigma) p(\sigma) - \gamma(\sigma) p_\sigma(\sigma)] u_\sigma^2 d\sigma \right). \quad (62)$$

From the structure of $\gamma(s)$ and $p(s)$, it is straightforward to show that

$$\gamma_s(s) p(s) - \gamma(s) p_s(s) = 1 + p(s); \quad (63)$$

hence, we can use (62) and (63) to construct the following upper bound for A_2:

$$A_2 \leq \beta \left(\gamma(1) p(1) u_s^2(1,t) - \int_0^1 p(\sigma) u_\sigma^2 \, d\sigma \right). \quad (64)$$

After substituting (59) and (64) into (55) and then substituting the resulting expression along with (54) into (50), we have

$$\dot{V} \leq -\left(\frac{p(1)}{2} - \beta\gamma(1) \right) u_t^2(1,t) - \left(\frac{p(1)}{2} - \beta\gamma(1) p(1) \right) u_s^2(1,t)) - \left(k_s - \frac{p(1)}{2} \right) \eta^2 - 2\beta E_s, \quad (65)$$

where (21) has been utilized. From (65) and (24), it is clear that if the controller gain k_s is selected according to (14) and the design constant β is selected according to

$$\beta < \min\left\{ \frac{p(1)}{2\gamma(1)}, \frac{1}{2\gamma(1)}, \frac{\min\{1, p\}}{4\gamma(1)} \right\}, \quad (66)$$

then $\dot{V}(t)$ can be upper bounded by the nonpositive scalar function given in (27).

LEMMA A.3. *If (i) $V_a(t)$ is a non-negative, scalar function which is lower bounded by zero, (ii) $\dot{V}_a(t) \leq -f(t)$ where $f(t)$ is a scalar, non-negative function, and (iii) $\dot{f}(t)$ is bounded then*

$$\lim_{t\to\infty} f(t) = 0. \quad (67)$$

Proof. First, we define the following function:

$$V_n(t) = V_a(t) - \int_0^t (\dot{V}_a(\tau) + f(\tau)) d\tau, \quad (68)$$

which is lower bounded by zero (since we have assumed that $V_a(t) \geq 0$ and that $\dot{V}_a(t) \leq -f(t)$, we know that $V_n(t) \geq 0$). If we differentiate (68) with respect to time, we obtain

$$\dot{V}_n(t) = -f(t). \quad (69)$$

We now apply a lemma from Slotine and Li (1991) (see page 127) which states that if: (i) $V_n(t)$ is a non-negative, scalar function which is lower bounded by zero, (ii) $\dot{V}_n(t) = -f(t)$ where $f(t)$ is a scalar, non-negative function, and (iii) $\dot{f}(t)$ is bounded then

$$\lim_{t\to\infty} f(t) = 0. \quad (70)$$

Application of the above lemma to (68) and (69) yields the result given by (67).